Spectroscopic Investigations of the Single Tryptophan Residue and of Riboflavin and 7-Oxolumazine Bound to Lumazine Apoprotein from *Photobacterium leiognathi*†

Tadeusz Kulinski‡ and Antonie J. W. G. Visser*
Department of Biochemistry, Agricultural University, 6703 BC Wageningen, The Netherlands
Dennis J. O'Kane and John Lee
Bioluminescence Laboratory, Department of Biochemistry, University of Georgia, Athens, Georgia 30602
Received July 16, 1986; Revised Manuscript Received October 7, 1986

ABSTRACT: Spectroscopic techniques have been applied to investigate the conformation, local structure, and dynamic properties of the apoprotein of the lumazine protein from *Photobacterium leiognathi* and the holoprotein reconstituted with either the natural ligand 6,7-dimethyl-8-ribityllumazine or the closely related analogues riboflavin and 6-methyl-7-oxo-8-ribityllumazine (7-oxolumazine). The analogues are bound similarly to the natural prosthetic group. They exhibit similar shifts on binding in their absorption and fluorescence spectra, single-exponential fluorescence decays, and no independent motion from the protein as evident from a long-lived anisotropy decay (single-exponential ϕ = 10 ns, 20 °C) and high initial anisotropy. Steady-state anisotropy measurements result in similar K_D's (40 nM, 20 °C, 50 mM inorganic phosphate) for all ligands. Circular dichroism in the far-UV region (190–250 nm) indicates no change in secondary structure on binding to the apoprotein. In the spectral region of 250–310 nm relatively large changes occur, indicating changes in the environment of the tyrosine and tryptophan residues. The single tryptophan residue shows a three-exponential decay of its fluorescence in both the apoprotein and the holoprotein. Radiationless energy transfer also occurs from the tryptophan to the bound ligand, especially evident with 7-oxolumazine. We have designed a new method for evaluation of the rate constant of energy transfer by measuring the (picosecond) rise time of the acceptor fluorescence. The anisotropy decay of the tryptophan residue shows two correlation times, a short one ($\phi \cong 0.4$ ns) representing rapid but restricted oscillation of this residue and a longer one (ϕ_2 = 5–7 ns, 20 °C) representing the motion of a larger segment of the protein.

Lumazine protein from the bioluminescent bacteria is a 21 200-dalton protein that has been well characterized with regard to its chemical and physical properties and emitting function (O'Kane et al., 1985; O'Kane & Lee, 1985a,b; Lee et al., 1985). The protein contains two chromophoric groups with spectral properties that can be utilized to obtain structural and dynamic information [for a survey see Visser and Lee (1987)]. Since the lumazine protein, isolated from the relatively thermophilic strain *Photobacterium leiognathi*, has its ligand tightly associated within the temperature range of 0–35 °C (Lee et al., 1985), the protein proves a good candidate for structural investigations with spectroscopic techniques.

Dissociation of the native prosthetic group can be performed with relatively mild methods (O'Kane & Lee, 1985a). The resulting apoprotein has binding capacity not only for 6,7-dimethyl-8-ribityllumazine, I, but also for the closely related compounds 6-methyl-7-oxo-8-ribityllumazine (7-oxolumazine, II) and riboflavin, III (see Chart I).

In fact, 7-oxolumazine is a probable oxidation product of 6,7-dimethyl-8-ribityllumazine photolysis (Lee, 1985). This last lumazine derivative is the precursor metabolite in prokaryotic riboflavin biosynthesis. The two analogues have therefore structural features in common with the native lumazine derivative. The compounds are fluorescent both on and off the protein.

Chart I

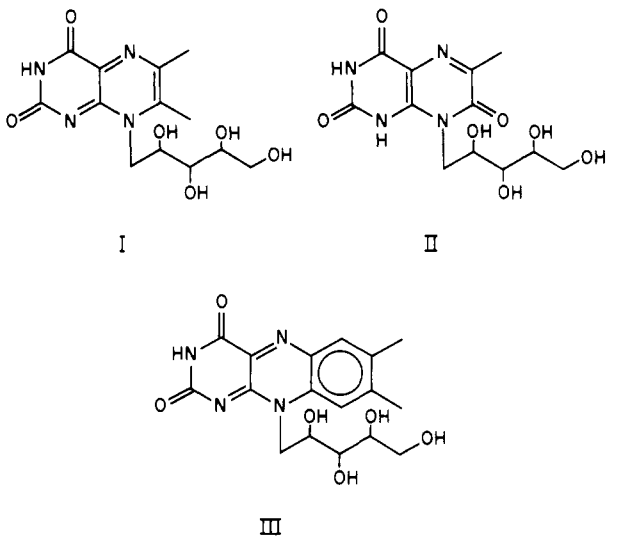

I II III

Fluorescence is the method of choice to obtain structural and thermodynamic information on the protein recombined with different ligands. Accessibility toward potassium iodide and ligand dissociation constants can be inferred from steady-state fluorescence methods (Visser & Lee, 1980, 1987; Lee et al., 1985). Results obtained with circular dichroism provide secondary structural details of the whole polypeptide chain and information on the microenvironment of aromatic residues and the ligand binding site.

Time-resolved fluorescence methods applied to proteins have now acquired maturity and reliability in obtaining dynamics

† Work supported by grants from the Netherlands Foundation for Chemical Research (S.O.N.) with financial aid from the Netherlands Organization for the Advancement of Pure Research (Z.W.O.) and by National Institutes of Health Grant GM 28139.
‡ On leave from the Institute of Bioorganic Chemistry, Polish Academy of Sciences, Poznán, Poland.

0006-2960/87/0426-0540$01.50/0

of biopolymers. Recent surveys provide detailed accounts (Lakowicz, 1983; Cundall & Dale, 1983; Beechem & Brand, 1985; Masotti & Szabo, 1987). We have applied these methods both to the fluorescent ligands and to the single tryptophan residue in the protein. The fluorescent analogues are tightly associated as is the ligand in the native lumazine protein. The tryptophan residue, however, exhibits rapid restricted motion, indicating that its local structure is less compact. We have taken advantage of the presence of two distinct chromophoric residues to obtain their separation from time-resolved fluorescence measurements in the different holoproteins. The internally consistent results obtained with the two lumazine derivatives prove very valuable in establishing this topology.

Materials and Methods

6,7-Dimethyl-8-ribityllumazine and 7-oxolumazine were gifts of Professor H. C. S. Wood (University of Strathclyde). Riboflavin and *N*-acetyltryptophanamide were obtained from Sigma. 2,2′-(*p*-Phenylene)bis[5-phenyloxazole] (POPOP)[1] was obtained from Eastman Kodak. *p*-Terphenyl was purchased from Fluka.

The isolation of homogeneous lumazine protein from *P. leiognathi* has been described previously (O'Kane et al., 1985). Unless otherwise indicated, a buffer of 50 mM phosphate and 5 mM 2-mercaptoethanol, pH 7.0, was used throughout (standard buffer). The concentration of lumazine protein was determined by using extinction coefficients as published earlier (Lee et al., 1985). Apoprotein was prepared according to the protocol of O'Kane and Lee (1985a), using a 0.5-mL column with DEAE-Sepharose 6B (Pharmacia). Lumazine apoprotein was eluted from the column with standard buffer containing 0.3 M potassium chloride. For far-UV circular dichroism (CD) measurements the protein was eluted with 50 mM phosphate containing 0.3 M potassium fluoride but without mercaptoethanol. Recombination was performed by addition of excess ligand, followed by ultrafiltration (Amicon Diaflo; YM10 membrane) or gel filtration (10-cm column of Bio-Gel P-6DG; Bio-Rad) to remove unbound ligand. Usually apoprotein preparation and recombination were performed a few hours preceding the measurements. Protein concentrations were in the range 0.1–1 μM, unless otherwise indicated.

Absorption and fluorescence spectra were obtained as previously described (Lee et al., 1985). Steady-state fluorescence anisotropy was measured with the photon-counting instrument described by Visser and Santema (1981). Emission was selected with Schott cutoff filters KV389, KV470, and KV500 for 7-oxolumazine, 6,7-dimethyl-8-ribityllumazine, and riboflavin, respectively.

Circular dichroism was obtained on a Jobin-Yvon Mark V autodichrograph (Agricultural University). For the far-UV region (190–250 mm) 1-mm path length cells were used, and for the UV/visible spectral region 10-mm cells were used. We have used a Fortran computer program to analyze the conformation of apo- and holoproteins, given a set of reference spectra. The basis for this analysis has been described elsewhere (Cantor & Schimmel, 1980). Three sets were used: the poly(L-lysine) reference spectra of Greenfield and Fasman (1969) and the basis sets of Saxena and Wetlaufer (1971) and Chen et al. (1974). Tests performed with CD spectra of human serum albumin and lysozyme, obtained with our instrument, resulted in the recovery of published structural contents.

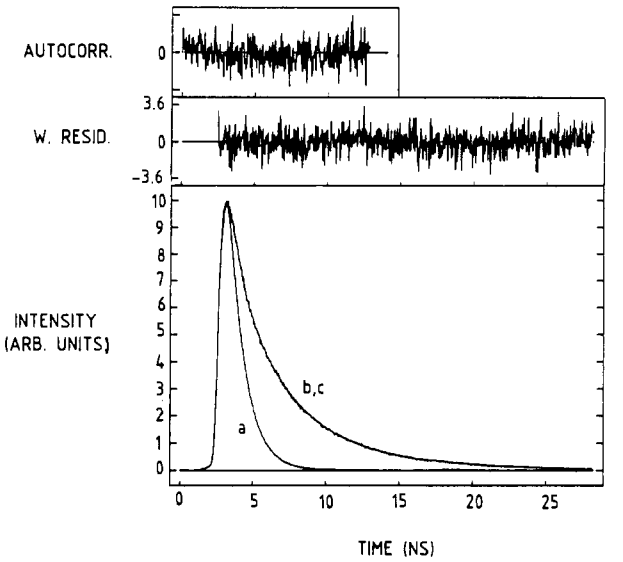

FIGURE 1: Total fluorescence decay of tryptophan in lumazine apoprotein at 20 °C. Three curves are presented: the fluorescence response of the reference compound *p*-terphenyl (a; τ_R = 1.06 ns) and experimental and calculated fluorescence decays (b, c). The fitted fluorescence decay consists of a triple-exponential function with lifetimes and relative amplitudes given in Table V. Also shown are the weighted residuals between calculated and experimental fluorescence and the autocorrelation function of the residuals. The first point of the autocorrelation function, equal to 1, has been omitted and the remainder of the function scaled to the maximum amplitude. The statistical parameters for this fit are χ^2 = 1.03 and Durbin–Watson parameter (Lampert et al., 1983) DW = 1.94. Time equivalence per channel is 31 ps.

Fluorescence decay and fluorescence anisotropy decay measurements were performed on the laser setup extensively described elsewhere (van Hoek & Visser, 1985; van Hoek et al., 1983; Visser & van Hoek, 1981; Visser et al., 1985). For tryptophan excitation a frequency-doubled, synchronously pumped rhodamine 6G dye laser output was used. Excitation wavelengths were at 295 and 300 nm, and emission was selected with a Baird-Atomic interference filter with maximum transmission at 344 nm or a Schott interference filter with transmission at 337 nm. Sensitized emission of ligands was measured through appropriate filters as described below for direct excitation. Free 7-oxolumazine and bound 7-oxolumazine were directly excited with the mode-locked output of the 363.8-nm line of an argon ion laser with UV optics (Visser & van Hoek, 1981). Fluorescence was viewed through a Balzers 437-nm or a Baird-Atomic 403 interference filter. Free riboflavin and bound riboflavin were directly excited with the mode-locked argon ion laser lines at 363.8 or 457.9 nm, and emission was selected with a Balzers 531-nm interference filter. Free 6,7-dimethyl-8-ribityllumazine and bound 6,7-dimethyl-8-ribityllumazine were excited at both 363.8 and 457.9 nm, with emission at 489 or 501 nm (Balzers). In all cases extracavity electrooptic modulators were used to reduce the laser repetition rate as described earlier (van Hoek & Visser, 1981, 1985; van Hoek et al., 1983).

Data analysis for fluorescence and anisotropy decay has been performed with a reference method to be described elsewhere (C. H. W. Vos and A. J. W. G. Visser, unpublished results). Suitable reference compounds for protein fluorescence are *N*-acetyltryptophanamide in water, pH 7, for which the fluorescence lifetime is 2.95 ± 0.03 ns at 20 °C (Chang et al., 1983), and *p*-terphenyl in ethanol [τ = 1.06 ns at 20 °C (Zuker

[1] Abbreviations: lumazine, 6,7-dimethyl-8-ribityllumazine; 7-oxolumazine, 6-methyl-7-oxo-8-ribityllumazine; lumP, lumazine protein; 7-oxolumP, 7-oxolumazine protein; POPOP, 2,2′-(*p*-phenylene)bis[5-phenyloxazole]; *Q*, quantum yield of fluorescence; Trp, tryptophan; ϕ, rotational correlation time; τ, fluorescence lifetime; CD, circular dichroism.

Table I: Analysis of Circular Dichroism in the Far-UV of Lumazine (Apo-) Protein from *P. leiognathi* (20 °C)

		basis set A[c]			basis set B[d]		
sample[a]	wavelenth range[b] (nm)	% α-helix	% β-sheet	% other	% α-helix	% β-sheet	% other
apoprotein 1	195–245	8	38	54	16	47	37
	200–245	8	44	48	17	49	33
	205–245	8	43	49	17	35	48
apoprotein 2	195–245	7	39	53	16	52	32
	200–245	8	40	52	14	59	37
	205–245	7	41	52	14	34	52
holoprotein 1	195–245	9	39	52	19	45	36
	200–245	9	45	46	20	49	31
	205–245	10	43	47	20	35	45
holoprotein 2	195–245	12	34	54	21	39	40
	200–245	12	43	45	24	45	31
	205–245	13	41	46	23	36	41

[a] Two different preparations of apoprotein and holoprotein were used. [b] Wavelength range of analysis. [c] Basis set of Saxena and Wetlaufer (1971). [d] Basis set of Chen et al. (1974).

et al., 1985)]. Examples of fluorescence and anisotropy decay analysis are illustrated for the lumazine apoprotein in Figures 1 and 2, respectively. For excitation at 300 and 363.8 nm and for monitoring emissions in the range 400–520 nm, the scintillator solute POPOP in ethanol can be used as reference compound, for which the lifetime is 1.3 ns at 20 °C (Zuker et al., 1985). For excitation at 457.9 nm and emission within 480–530 nm, data analysis was performed as previously described (Visser et al., 1985).

Results and Discussion

Circular Dichroism. A summary of the results is presented in Figure 3. Figure 3A gives the spectra of lumazine protein and its apoprotein in the region of 195–250 nm. It is apparent that neither spectrum shows the two distinct minima indicating the presence of much α-helix like that occurring in human serum albumin (50%). The results of the analysis described under Materials and Methods are collected in Table I. Similar results (not shown) as presented in Table I have been obtained with apoprotein reconstituted with 7-oxolumazine and riboflavin. It is concluded that there are no measurable differences in secondary structure between apo- and holoproteins. It is also evident that the basis sets of Saxena and Wetlaufer (1971) and Chen et al. (1974) lead to more congruent results, especially when the range of wavelengths is narrowed. The basis set of Greenfield and Fasman (1969) resulted in inconsistent structural parameters, which are omitted in Table I. It should be noted that the results obtained with the basis set of Chen et al. (1974) are biased toward more helix content. The more quantitative method of Hennessey and Johnson (1981) was not used in this comparative study.

Bound riboflavin (Figure 3B) shows an intensified negative Cotton effect (at 450 nm) comparable to that of lumazine protein (-40×10^{-3} deg cm^2 dmol^{-1} at 420 nm; Lee et al., 1985). The second absorption band shows enhanced positive dichroism in bound riboflavin, which does not coincide completely with the slightly positive band in free riboflavin. Edmondson and Tollin (1971) found the same tendency for ferredoxin–NADP$^+$ reductase, although the rotational strength of the second absorption band is larger than that of the first electronic transition in that flavoprotein. The situation is opposite from that found in flavodoxin, where the first absorption band exhibits positive dichroism and the second absorption band negative dichroism (Edmondson & Tollin, 1971). This distinction must be caused by specific differences in the flavin binding region, which are reflected in different symmetries of the two lowest electronic transitions. The aromatic amino acid region exhibits a characteristic dispersive band between 250 and 300 nm, which must be caused by opposite contributions of ligand and aromatic amino acids.

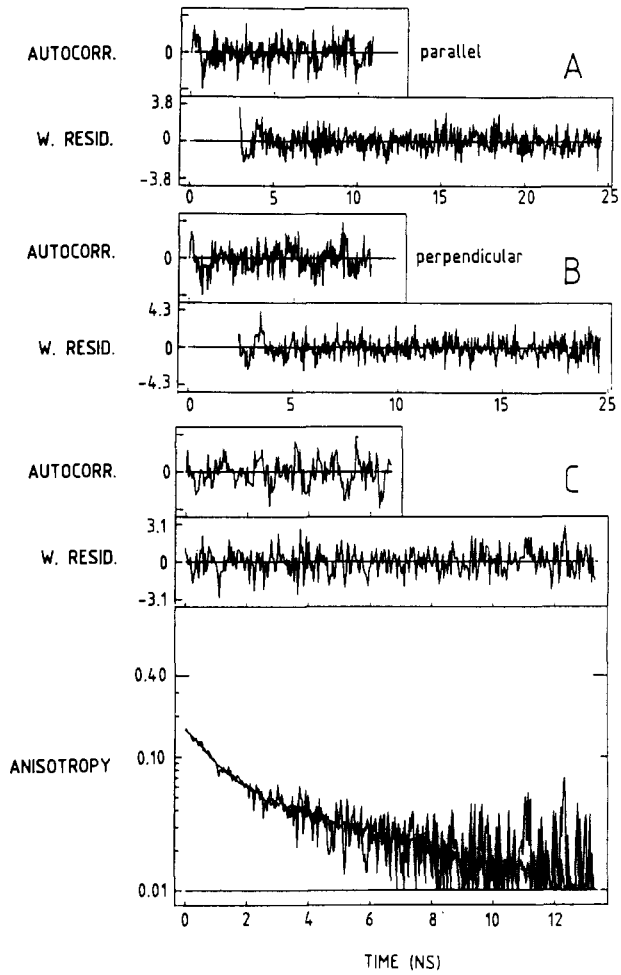

FIGURE 2: Example of fluorescence anisotropy decay analysis of tryptophan in apolumazine protein at 20 °C. The parallel and perpendicular polarization components of the fluorescence were simultaneously fitted to a biexponential decay model. In panels A and B the weighted residuals and autocorrelation functions for this fit are presented. The correlation times and their amplitudes are given in Table V. The statistical parameters for this fit are $\chi^2 = 1.17$ and DW = 1.84 (see legend of Figure 1 for details). Panel C shows a replot of a portion of the experimental and calculated anisotropy decays with associated weighted residuals and autocorrelation function. Statistical parameters and weighted residuals were recalculated according to Wahl (1979), $\chi^2 = 1.12$, and DW = 2.20.

Figure 3C presents the CD spectrum of the apoprotein between 250 and 350 nm, in which a negative Cotton effect

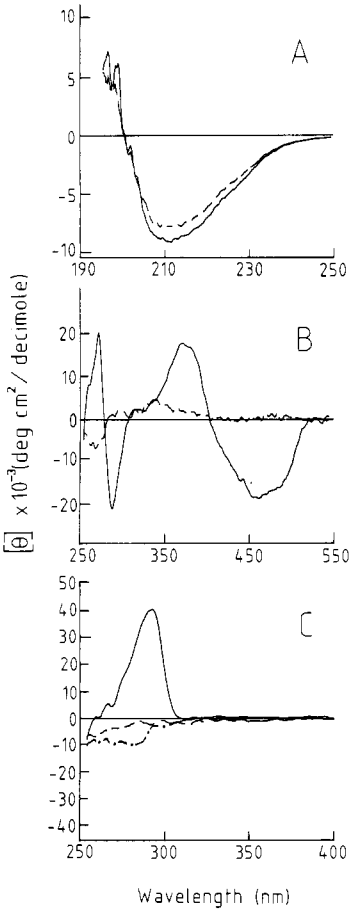

FIGURE 3: Circular dichroism spectra of lumazine protein and apoprotein alone (panel A) and reconstituted with riboflavin (panel B) and 7-oxolumazine (panel C). (A) The mean residual ellipticity is shown, based on 196 amino acids (O'Kane & Lee, 1985a). Lumazine protein (—) and apoprotein (---), 12 μM. (B) Free (---) and protein-bound riboflavin (—), 10 μM. (C) Free (---) and protein-bound 7-oxolumazine (—), 15 μM. The spectrum of the apoprotein (·–·), 15 μM, is shown for comparison.

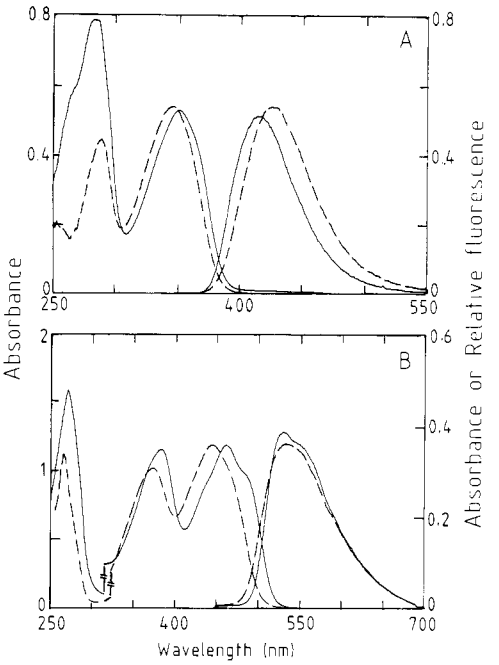

FIGURE 4: Absorption and fluorescence spectra of ligands free and bound to lumazine apoprotein. (A) Free (---) and protein-bound (—) 7-oxolumazine. (B) Free (---) and protein-bound (—) riboflavin. The left scale refers to the part of the spectra at the left.

Table II: Fluorescence Properties of 7-Oxolumazine, Riboflavin, and 6,7-Dimethyl-8-ribityllumazine (Lumazine) Free and Bound to Lumazine Apoprotein (P) at 20 °C

sample[a]	excitation λ_{max} (nm)[b]	emission λ_{max} (nm)	Q_F	k_q (10^9 M^{-1} s^{-1})[c]
7-oxolumazine	345	424	0.91[d]	3.3
7-oxolumazine–P	350	419	0.95[d]	1.2
riboflavin	370, 445	525	0.26[e]	16.7
riboflavin–P	385, 465	530	0.30	9.0
lumazine[f]	408	490	0.45	6.2
lumazine–P	420	475	0.54	1.6

[a] Protein concentrations in the range 1–10 μM. [b] From absorption and corrected excitation spectra. [c] From the Stern–Volmer constant $K_{SV} = k_q\tau_0 = (F_0/F - 1)/[KI]$, where F_0 is the fluorescence intensity in the absence of KI, F is the fluorescence intensity in the presence of KI, and τ_0 is from Table III. [d] Relative to quinine sulfate in 1 N H_2SO_4, $Q_F = 0.52$. [e] From Weber and Teale (1957). [f] From Lee et al. (1985).

can be observed. The 7-oxolumazine protein shows a strongly positive Cotton effect similar to native lumazine protein (Lee et al., 1985) in this spectral region. 7-Oxolumazine itself has a small negative dichroism below 300 nm. The positive dichroism of this electronic transition of bound 7-oxolumazine must be strongly induced by the asymmetric environment. In contrast to riboflavin and lumazine, the bound 7-oxolumazine does not show enhanced dichroism at the lowest energy absorption band of the ligand. This absence must be due to the intrinsic weak rotational strength of this electronic transition of 7-oxolumazine, which possesses local symmetry (cf. Chart I).

Fluorescence Properties. In Figure 4 the absorption and fluorescence spectra of free and bound 7-oxolumazine and riboflavin are shown. The spectra of 7-oxolumazine exhibit the same characteristic features as those encountered in lumazine protein. The absorption maximum of free 7-oxolumazine is at 345 nm, and that of the bound is at 350 nm. The wavelength of maximum emission for free is 424 nm, and that for bound is 419 nm. The two absorption bands of riboflavin show bathochromism in the bound case (465 and 385 nm) as compared to the free case (445 and 370 nm). The fluorescence maxima of free and bound are in the same range: 525–535 nm. These spectral results, together with quantum yields, have been collected in Table II. For comparison we have collected results obtained with reconstituted lumazine protein. It is evident that there are no differences between native and reconstituted lumazine protein.

Figure 5 gives examples of fluorescence decays of protein-bound analogues. The decays are in all cases (free or bound) exponential, and the results are in Table III. There are no dramatic changes in relative quantum yield or in the lifetime when free and bound ligands are compared. It is also apparent from data in Table III that native and reconstituted lumazine proteins are indistinguishable.

Exposure of bound aromatic ligands was tested with collisional fluorescence quenching by potassium iodide. A linear Stern–Volmer relation is observed with concentrations of potassium iodide up to 0.1 M. In Table II we have listed the rate constants for quenching k_q obtained from the ratio K_{SV}/τ_0, where K_{SV} is the Stern–Volmer constant and τ_0 is the fluorescence lifetime in the absence of potassium iodide. The data for recombined lumazine protein are again similar to the ones for native lumazine protein (Lee et al., 1985). The similarity of the k_q for the bound analogues, within a factor of 2–3, is striking and implies an almost complete exposure to the quencher molecules.

Steady-state fluorescence polarization has been proven to yield equilibrium concentrations of free and bound ligands in

Table III: Fluorescence Lifetimes and Rotational Correlation Times of 7-Oxolumazine, 6,7-Dimethyl-8-ribityllumazine (Lumazine), and Riboflavin Free or Bound to Lumazine Apoprotein (P) from *P. leiognathi*

	T (°C)	λ_{ex} (nm)	λ_{em} (nm)	α_1	τ_1 (ns)	α_2	τ_2 (ns)	r_0 ($=\beta_1$)	ϕ (ns)
7-oxolumazine	20	363.8	437	1.0	7.10			0.12	0.11
7-oxolumazine-P	20	363.8	437	1.0	7.48			0.30	9.9
7-oxolumazine-P	20	300	403	1.12	7.32	−0.12	0.66	−0.046	8.9
7-oxolumazine-P	5	295	403	1.0	7.40			−0.10	14.0
riboflavin	20	363.8	531	1.0	4.68			0.09	0.18
riboflavin-P	20	363.8	531	1.0	5.83			0.18	9.8
riboflavin-P[a]	20	457.9	531	0.42	5.5	0.58	4.8	0.22	0.18[b]
								0.16	11.0
lumazine	20	363.8	501	1.0	9.20			0.13	0.13
lumazine-P	20	363.8	501	1.0	14.69			0.27	12.2
lumazine-P	20	300	489	1.53	14.30	−0.53	1.14	−0.016	14.4

[a] Dilute protein solution (80 nM), lifetimes fixed to values indicated. [b] Anisotropy decay, two-component analysis.

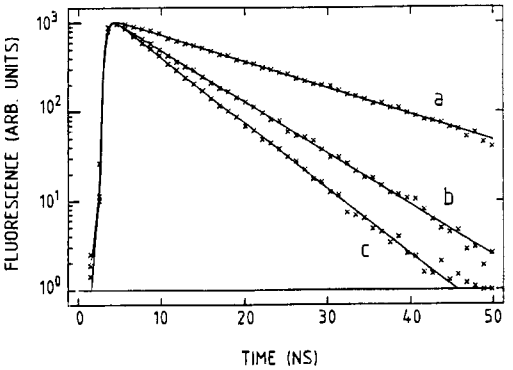

FIGURE 5: Fluorescence decays of apoprotein reconstituted with respectively lumazine (a), 7-oxolumazine (b), and riboflavin (c). (×) denotes each tenth experimental point, and the solid line indicates the single-exponential fit to the data. The excitation wavelength is 363.8 nm, and the recovered fluorescence lifetimes are presented in Table III.

ligand–protein complexes (Chien & Weber, 1973). The dissociation constant can be obtained from the relationship

$$K_D = c[(I_b/I_f)(1 - p/p_b)]^2/[1 - (1 - p/p_b)] \quad (1)$$

where c is the total concentration of free and bound ligand; I_b/I_f is the ratio of bound to free ligand fluorescence intensities and can in the first approximation be set equal to τ_b/τ_f, where τ_b and τ_f are the fluorescence lifetimes for bound and free ligand, respectively; and p_b is the polarization when all the ligand is bound. It can be equated to the value of the fluorescence polarization at high protein concentration or determined as described by Visser and Lee (1980).

In Table IV the results have been collected. It is unambiguously shown that the ligands are tightly associated, exemplified by the low dissociation constants. The K_D of reconstituted lumazine protein is similar to the one obtained previously (Lee et al., 1985). It should be noted that the K_D values are extremely sensitive to the adopted values of I_b/I_f and p_b. Combining the results, we obtain the following values: for riboflavin, $K_D = 36 \pm 41$ nM (5 observations): for 7-oxolumazine, $K_D = 35 \pm 19$ nM (11 observations). Judging from the significant spread in the values, we have to conclude that the binding to the apoprotein is equally strong for the three ligands.

Inflexible attachment is also apparent from fluorescence anisotropy decay patterns as shown in Figure 6. In these examples the decay is exponential with single rotational correlation times as given in Table III.

In Table III we also incorporated the results of a dilution experiment using the protein recombined with riboflavin. Especially the anisotropy decay is clearly biexponential with a very short (0.18-ns) and a long (11.0-ns) correlation time.

Table IV: Steady-State Fluorescence Polarization (p) and Dissociation Constant (K_D) of 7-Oxolumazine, 6,7-Dimethyl-8-ribityllumazine (Lumazine), and Riboflavin Bound to Lumazine Apoprotein (P) from *P. leiognathi* (20 °C)

sample	concn (nM)	p	K_D[a] (nM)
7-oxolumazine-P	6500	0.258	
	980	0.253	
	650	0.232	3
	490	0.221	7
	330	0.192	24
	230	0.182	24
	160	0.148	48
	120	0.140	45
	80	0.140	45
	60	0.110	40
	40	0.092	50
7-oxolumazine	40–6500	0.007 ± 0.003	
lumazine-P[b]	3600	0.216	
	1800	0.217	13
	900	0.196	52
	220	0.146	131
	110	0.143	73
lumazine	110–3600	0.007 ± 0.003	
riboflavin-P	2200	0.308	
	550	0.286	
	270	0.258	7
	135	0.235	10
	60	0.176	29
	34	0.153	25
	17	0.072	100
riboflavin	17–2200	0.021 ● 0.010	

[a] Calculated with the following parameters: for 7-oxolumazine, $I_b/I_f = 1.04$, $p_b = 0.248$; for lumazine, $I_b/I_f = 1.45$, $p_b = 0.230$ (Lee et al., 1985); for riboflavin, $I_b/I_f = 1.16$, $p_b = 0.297$. [b] Recombined.

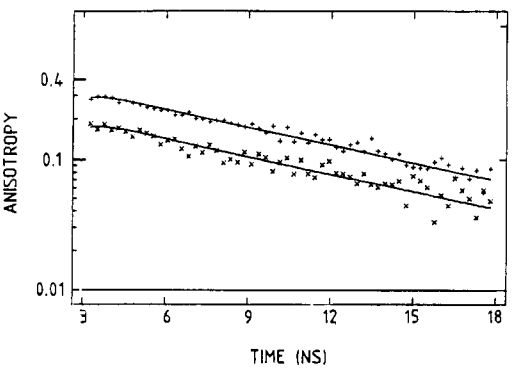

FIGURE 6: Fluorescence anisotropy decay of 7-oxolumazine (+) and riboflavin (×) bound to lumazine apoprotein. The excitation wavelength is 363.8 nm. Every fifth experimental point is presented. The solid lines are fits with single correlation times (see Table III for values). The time scale refers to the time scale in Figure 5.

The fluorescence decay is also biexponential, but the two lifetimes are closely spaced, which forced us to fix the two

lifetimes to those of free and bound riboflavin in the analysis. Visser and Lee (1987) have provided the protocols for measuring the relative concentrations of free (c_f) and bound (c_b) ligands. Since the excitation at 458 nm is near an isosbestic point in the absorption spectrum (Figure 4B), it can be shown that $c_f/c_b = \alpha_f\tau_f/(\alpha_b\tau_b)$, where α_f and α_b are the amplitudes in the biexponential decay. Substituting the values of Table III, we find $c_f/c_b = 1.21$, and with the 80 nm protein solution this means that $K_D = 43.8$ nM. Similarly, it follows from the anisotropy at $t = 0$ that $c_f/c_b = 0.22/0.16 = 1.38$, which yields $K_D = 46.4$ nM. The values are in excellent agreement with those from steady-state fluorescence polarization, but it should be noted that the former were obtained from a single experiment.

Rotational correlation times obtained for emission anisotropy of ligands bound to protein together with results of free ligands excited at different wavelengths are presented in Table III. For all chromophores bound to the protein the fluorescence anisotropy decay shows single-exponential behavior, but rotational correlation times obtained for different chromophores at different excitation wavelengths are slightly different. The initial anisotropies are high when excitation is within the first electronic absorption band. Smaller or even negative initial anisotropies are observed when the excitation is in higher electronic transitions.

Fluorescence anisotropy decay is described by a single correlation time only in the case of spherical bodies. For ellipsoids of revolution (and practically for asymmetric bodies) the emission anisotropy $r(t)$ is a sum of three exponentials instead of five components as predicted by the theory (Belford et al., 1972; Chuang & Eisenthal, 1972; Ehrenberg & Rigler, 1972; Small & Isenberg, 1977):

$$r(t) = \sum_{i=1}^{n} \beta_i \exp(-t/\phi_i) \qquad (2)$$

where the preexponential factors depend on the relative orientation between the transition moments of the molecule and the symmetry axis of the rotating particle. Experimentally, analysis of the decay of anisotropy for anisotropic rotators often yields almost the same statistical criteria for the assumption of monoexponential and biexponential functions (Barkley et al., 1981a). Such an experimental difficulty may probably be diminished but not removed by improvement of experimental and analytical procedures.

Another way to increase the information content of rotational relaxation processes available from fluorescence anisotropy has been proposed by Barkley et al. (1981b). It is based on the excitation into different electronic transitions of the chromophore, creating another initial distribution of emission dipoles due to differently oriented absorption transition moments. The dependence of the rotational correlation times on the excitation wavelength, recovered after a one-component analysis, provides the evidence for more complex anisotropy decay.

Rotational correlation times, obtained for different excitation conditions for the investigated chromophores bound to the protein, show some evident differences, suggesting that lumazine protein is not an isotropic rotator but shows some anisotropic motion. The apparent parameters obtained from monoexponential analysis are effective averages of the true parameters of the multiexponential decay, but double-exponential analysis gives the same statistical criteria for the quality of fitting for different components. For the detailed analysis, knowledge of the location of the transition dipole directions relative to the diffusion principal axes of the macromolecule is necessary. Up to now, we can only estimate the anisotropy of the shape of the macromolecule by simple speculation, using a model of prolate ellipsoid of revolution for the protein. We may assume that the longest rotational correlation time approaches the value of the rotational correlation time associated with the reorientational motion of the longer axis of the prolate ellipsoid of revolution. The shorter correlation time, measured with another orientation of the transition moment, will be a superposition of correlation times associated with both rotations around an axis perpendicular to the symmetry axis and around the symmetry axis. Then this short effective relaxation time will be the highest limiting value for the correlation time for the rotations around the symmetry axis of the protein. Then $\phi_{max} = 11$ ns for excitation of lumazine at 458 nm (Lee et al., 1985), and $\phi_{min} = 8.9$ ns for excitation of 7-oxolumazine at 300 nm at 20 °C. The limiting ratio $\phi_{min}/\phi_{max} \cong 0.80$ corresponds to the ratio of rotational correlation times for a prolate ellipsoid of revolution with an axial ratio of 1.25 (Koenig, 1974). The real anisotropy of the shape of the molecule should exceed this value. The result corresponds well with data obtained with other techniques for lumazine protein (O'Kane & Lee, 1985b). Excitation at 300 nm and monitoring lumazine fluorescence at 489 nm result, after single-exponential analysis, in a relatively long correlation time with low initial anisotropy (Table III). This must be due to a superposition of anisotropies contributed by direct excitation and substantial excitation via energy transfer from tryptophan.

Time-Dependent Tryptophan Fluorescence. In Table V the results of tryptophan fluorescence decay in apoprotein and reconstituted proteins are summarized. From comparison with the results on the apoprotein (Figure 1) two conclusions can be drawn. First, the decay is highly nonexponential in both proteins. A minimum decay model is that of a sum of three exponential terms. Previously, we have fitted tryptophan fluorescence in lumazine protein with two lifetimes, but that resulted in relatively poor fits (Lee et al., 1985). Second, the presence of fluorescent ligands in the protein gives rise to more rapid decay. This effect must be caused by energy transfer from tryptophan to ligands, providing an extra decay channel for the tryptophan (donor) fluorescence. For tryptophan fluorescence in 7-oxolumazine protein a four-component fit was required, in which the fourth component correlated perfectly with the fluorescence lifetime of protein-bound 7-oxolumazine. The fluorescence of 7-oxolumazine still interferes at its leading edge, even at 337 nm, with the spectrum of tryptophan fluorescence excited at 300 nm. Therefore, this exponential component is not taken into account in the estimation of the tryptophan fluorescence lifetime. Note in this respect the large quantum yield (0.95, Table II) of the 7-oxolumazine fluorescence.

The recovered lifetimes show a very characteristic pattern. In all preparations a short (0.1–0.6 ns), a medium (1.1–3.6 ns), and a long lifetime component (6.1–6.6 ns at 5 °C) can be distinguished. The long component has the largest contribution in the apoprotein at 5 °C, yielding the longest average lifetime. The short component has generally more contribution in the holoproteins.

Chang et al. (1983) and Petrich et al. (1983) suggest a quenching mechanism of the indole residue in tryptophan-containing peptides by charge transfer of indole to an adjacent electrophilic carbonyl involving the protonated amine and leading to more efficient nonradiative decay. The short and medium components are assigned to distinct rotamers [see also Szabo and Rayner (1980)], in which indole, carbonyl, and protonated amine are positioned at a certain distance and orientation. The long component arises from a conformer in

Table V: Tryptophan Fluorescence Lifetimes and Correlation Times in Apoproteins and Reconstituted Proteins of Lumazine Protein from *P. leiognathi*[a]

sample	T (°C)	α_1	$\tau_1 \pm 0.05$ (ns)	α_2	$\tau_2 \pm 0.1$ (ns)	α_3	$\tau_3 \pm 0.1$ (ns)	$\bar{\tau}$[b] (ns)	β_1	$\phi_1 \pm 0.05$ (ns)	β_2	$\phi_2 \pm 0.1$ (ns)	$r(0)$[c]	τ_{eff} (ns)	D_w (ps^{-1})	D_p (ps^{-1})	θ_0 (deg)
lumP	5	0.45	0.50	0.40	1.6	0.15	6.1	1.8	0.09	0.51	0.11	8.2	0.20	0.54	175	20	35
	20	0.47	0.40	0.34	1.5	0.18	4.3	1.5	0.10	0.30	0.07	5.0	0.17	0.32	409	33	43
	35	0.50	0.36	0.33	1.4	0.17	3.9	1.3	0.10	0.30	0.04	5.5	0.14	0.32	526	30	49
apo-P	5	0.45	0.62	0.30	3.6	0.25	6.7	3.8	0.10	0.53	0.10	8.4	0.20	0.57	193	20	38
	20	0.41	0.59	0.36	2.8	0.22	5.8	2.5	0.12	0.47	0.07	6.0	0.19	0.51	284	28	45
	35	0.33	0.42	0.50	2.3	0.17	4.8	2.1	0.09	0.30	0.03	8.7	0.12	0.31	573	19	52
7-oxo-lumP	5	0.80	0.10	0.10	3.1	0.10	6.0	1.0	0.095	0.35	0.08	5.5	0.175	0.37	319	30	40
	20	0.82	0.10	0.10	2.9	0.28	5.7	0.8	0.10	0.31	0.05	5.0	0.15	0.33	413	33	45
	35	0.85	0.08	0.06	2.4	0.09	4.1	0.7									
riboflavin-P	5	0.57	0.39	0.29	1.1	0.14	6.0	1.4	0.09	0.44	0.08	6.6	0.17	0.47	256	25	39
	35	0.53	0.30	0.39	1.1	0.08	5.9	1.1	0.09	0.33	0.05	8.7	0.14	0.34	441	19	45

[a] Excitation at 300 nm; emission at 337 nm. [b] $\bar{\tau} = (\sum_{i=1}^{3} \alpha_i \tau_i)/(\sum_{i=1}^{3} \alpha_i)$. [c] Anisotropy at $t = 0$.

which indole is distant from carbonyl and/or protonated amine. In addition, Gudgin-Templeton and Ware (1984) demonstrated the important role of excited-state complexation with the solvent in explaining the photophysics of tryptophan. Following extrapolation of these possibilities to the single tryptophan residue in lumazine protein, the results must be interpreted by the presence of various tryptophan environments.

Table V also accommodates the results of anisotropy decay analysis of the single tryptophan residue in apo- and holoproteins. Excitation at 300 nm yields higher initial anisotropies than at 295 nm, since the ^1L_a transition is more exclusively excited at 300 nm (Valeur & Weber, 1977). The decay can be best described with two correlation times as reported earlier for the holoprotein (Lee et al., 1985). The short correlation time is in the range 0.3–0.5 ns, while the longer one is in the range 5.0–9.0 ns depending on the temperature. The results presented in Table V differ slightly from the previous values (Lee et al., 1985). However, it should be stressed that the excitation/emission conditions were different. The short component can be ascribed to local tryptophan motions and the longer one to larger segmental rotation. Interestingly, the short component shows no temperature dependence, indicating that this local motion hardly has an activation barrier.

Lipari and Szabo (1980) have derived an approximate expression for this wobbling in cone motion (assuming that either absorption or emission transition moments point along the axis that wobbles):

$$r(t)/r(0) = (1 - A_\infty) \exp[-t(\tau_p^{-1} + \tau_{eff}^{-1})] + A_\infty \exp(-t/\tau_p) \quad (3)$$

$$\tau_p = (6D_p)^{-1} \quad (4)$$

where D_p is the rotational diffusion coefficient of the protein, τ_{eff} is related to D_w, the wobbling diffusion constant, and

$$A_\infty = \beta_2/r(0) = [\tfrac{1}{2}(\cos\theta_0)(1 + \cos\theta_0)]^2 \quad (5)$$

where θ_0 is the cone angle. The data in Table V are sufficient to derive θ_0, $\tau_p(=\phi_2)$, D_p, τ_{eff}, and D_w by following the procedure given by Lipari and Szabo (1980). These estimates are also incorporated in Table V. It can be easily seen that D_w increases with increasing temperature, and this is connected with a larger cone angle over which the tryptophan is moving.

Energy Transfer from Tryptophan to the Ligand. As is shown in Table V, the binding of ligands to the protein induces a significant shortening of the tryptophan fluorescence decay time. Analysis of the spectral overlap between the fluorescence band of the tryptophan residue and the absorption bands of ligand, presented in Figure 7, confirms that the value of the spectral overlap integral J is not small, especially for 7-oxolumazine, and this gives rise to important nonradiative energy transfer between tryptophan and ligands. When nonradiative energy transfer takes place, the fluorescence lifetime of the donor τ_D obeys the relation (Steinberg, 1971);

$$1/\tau_D = 1/\tau_{D_0} + k_{DA} \quad (6)$$

where τ_{D_0} is the lifetime of the donor fluorescence in the absence of acceptor. The rate of energy transfer k_{DA} between donor (D) and acceptor (A) is described by the well-known equation (Steinberg, 1971):

$$k_{DA} = 1/\tau_{D_0}(R_0/R)^6 \quad (7)$$

R is the distance between the donor and acceptor, and R_0 is the critical transfer distance given by the equation:

$$R_0^6 = (8.8 \times 10^{-25}) Q\kappa^2 n^{-4} J \quad (8)$$

Table VI: Energy-Transfer Parameters for the System Tryptophan (Donor) and Lumazine or 7-Oxolumazine (Acceptors) in Lumazine (or 7-Oxolumazine) Protein from *P. leiognathi* (20 °C)

acceptor	$10^{15}J$ (cm^6/mol)	θ^a (deg)	$\kappa_{min}^{2\,b}$	$\kappa_{max}^{2\,b}$	$R_{0_{min}}{}^c$ (Å)	$R_{0_{max}}{}^c$ (Å)	$10^9\tau_{DA}{}^d$ (s)	$R_{min}{}^e$ (Å)	$R_{max}{}^e$ (Å)	$10^9\tau_{DA}{}^f$ (s)	$R'_{min}{}^g$ (Å)	$R'_{max}{}^g$ (Å)
lumazine	2.78	0	0.65	2.7	17.7	22.5	1.50	18.4	23.4	1.10	16.7	22.7
		90	0.18	0.7	14.3	17.9		14.9	18.6		13.4	16.8
7-oxolumazine	10.48	0	0.81	2.4	22.9	27.5	0.85	20.2	24.2	0.66	19.0	22.8
		90	0.21	0.6	18.3	21.8		16.1	19.2		15.2	18.1

[a] θ is the angle that the transition moment of the fixed acceptor makes to the separation vector [cf. Dale and Eisinger (1974)]. [b] Estimated from graphs of Dale and Eisinger (1974); surface distribution and cone angles θ_0 of tryptophan were obtained from Table V. [c] From $R_0^6 = (8.8 \times 10^{25})Q\kappa^2 n^{-4} J$; J is the overlap integral, the quantum yield of the donor fluorescence Q is 0.1 (Lee et al., 1985), and the index of refraction n is 1.5 (Eisinger et al., 1969). [d] Calculated from fluorescence decay of tryptophan in the presence of ligands in protein from eq 11 (Table V). [e] Calculated from eq 9, 11, and 13 with τ_{DA} measured from tryptophan fluorescence decay, $\tau_{D_0} = 2.5$ ns. [f] Fluorescence lifetime of the donor (tryptophan) measured by fluorescence "growing in" of acceptor. [g] Calculated as in footnote *e* with τ_{DA} measured from sensitized fluorescence of acceptor.

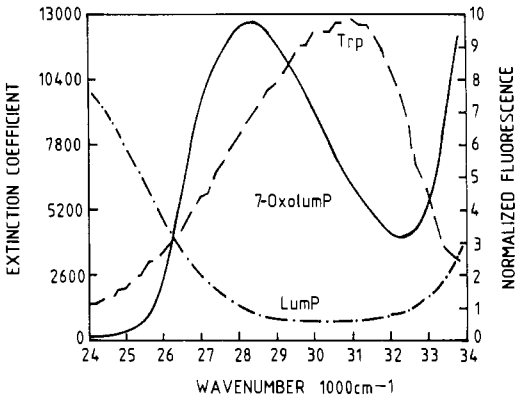

FIGURE 7: Spectral overlap between tryptophan fluorescence (Trp, ---) and light absorption of lumazine protein (lumP, ·–·) or 7-oxolumazine protein (7-oxo-lumP, —). The extinction coefficient for 7-oxolumazine at 28 571 cm^{-1} (ϵ' = 12 800 M^{-1} cm^{-1}) was taken from Rowan and Wood (1968).

where n is the refractive index of the surrounding medium, Q is the quantum yield of the donor fluorescence in the absence of the acceptor, and κ^2 is the orientation factor. For nonexponential fluorescence decays, as is the case of tryptophan in proteins, it is difficult to relate the fluorescence lifetimes to the rate of energy transfer. In addition, the energy-transfer rate may be influenced by static and dynamic mobility of macromolecules (Haas et al., 1978). Then the simple measurable quantity is the energy transfer efficiency E:

$$E = 1 - Q_{DA}/Q_D \tag{9}$$

where Q denotes relative fluorescence yield in the absence (Q_D) or presence (Q_{DA}) of acceptor, representing the photon flux integrated over time and different conformations. When the fluorescence intensity is described by a multiexponential function, then

$$F \sim \sum_{i=1}^{n} \alpha_i \exp(-t/\tau_i) \tag{10}$$

$$Q \sim \int_0^\infty \sum_{i=1}^{n} \alpha_i \exp(-t/\tau_i)\, dt = \sum_{i=1}^{n} \alpha_i \tau_i = \bar{\tau} \tag{11}$$

where α_i values are the normalized contributions of each exponential component. This shows that, by considering fluorescence efficiency, a weighted average fluorescence lifetime $\bar{\tau}$ defined in eq 11 should be used. The use of fluorescence lifetimes defined by

$$\bar{\tau} = \sum_{i=1}^{n} \alpha_i \tau_i^2 / \sum_{i=1}^{n} \alpha_i \tau_i \tag{12}$$

leads to wrong conclusions, especially when short lifetime components have an important contribution in the total fluorescence decay (as, for example, for 7-oxolumazine, Table V).

On the other hand, for a single donor–acceptor pair the transfer efficiency is equal to

$$E = 1/[1 + (R/R_0)^6] \tag{13}$$

and it is possible by combining eq 9 and 13 to estimate the distance between donor and acceptor by an analysis of complex fluorescence decay. Table VI presents different relevant energy-transfer parameters for the system tryptophan–ligand in the protein recombined with the two lumazine derivatives.

Dale and Eisinger (1974) have critically evaluated the orientation and dynamic depolarization factors for various models of donor–acceptor systems. In our case we have one tightly associated chromophore (6,7-dimethyl-8-ribityllumazine or 7-oxolumazine), while the other (tryptophan) is free to reorient over the surface or volume of a cone with a certain semiangle [model 3 of Dale and Eisinger (1974)]. Librational motions of the tryptophan within a certain cone angle have been obtained from time-resolved fluorescence depolarization (see previous section). In apo- and holoproteins the cone angles are on the order of 45°. This restricts the possible values for the orientation factor, as can be deduced from the graphical results of Dale and Eisinger (1974). In Table VI we have given maximum and minimum values for the orientation factor in the case of a distribution on the surface of a cone of the donor molecule for two possible angles θ that the separation vector makes to the fixed acceptor transition moment. The agreement between the two different acceptor molecules is excellent. The distance between the two chromophores is confined between 13 and 22 Å, depending on the exact value of the orientation factor. The determined Stokes radius of the protein is 22 Å (O'Kane & Lee, 1985b).

When tryptophan is excited and ligand fluorescence is monitored, the remarkable result is that there is a distinct buildup of acceptor fluorescence (see Figure 8 and results in Table III). It has been shown previously (Birks, 1970) that the time dependence of the acceptor fluorescence F_A excited via the donor can be described by

$$F_A(t) \sim (1/\tau_A - 1/\tau_D)^{-1} [\exp(-t/\tau_A) - \exp(-t/\tau_D)] \tag{14}$$

This equation is valid when there is no direct excitation of the acceptor. In practice this is seldom true, and the net effect would be a larger weight of the exponential containing the acceptor fluorescence lifetime τ_A. In effect, for 7-oxolumazine protein almost 85% of molecules are directly excited into the second absorption band, and the remaining 15% are excited through an energy-transfer process exhibiting fluorescence decay with evident "growing in". For lumazine this ratio is more in favor of an energy-transfer excitation mechanism. The short lifetime component with negative amplitude corresponds almost perfectly to the reciprocal energy-transfer rate esti-

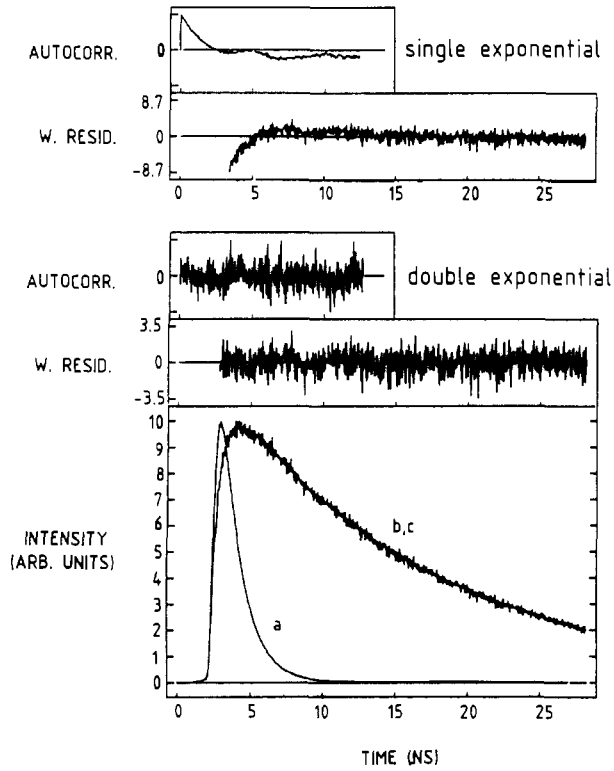

FIGURE 8: Fluorescence decay analysis of lumazine protein excited at 300 nm showing the partial buildup of fluorescence at 489 nm. The lower panel presents the two-exponential fit with parameters as in Table III. Curve a is the POPOP fluorescence response (τ_R = 1.30 ns). Curves b and c are experimental and calculated fluorescence decays, respectively. Further details are given in the legend of Figure 1. Statistical parameters: χ^2 = 1.20, DW = 2.06. The upper panel shows the weighted residuals and autocorrelation function for a single-exponential fit with the following results: τ = 15.1 ns, χ^2 = 2.50, and DW = 0.84.

mated with eq 6. Agreement between energy-transfer parameters and distances derived both with tryptophan fluorescence lifetime shortening and with acceptor fluorescence "growing in" presented in Table VI confirms that this last experimental method may represent an alternative approach in energy-transfer measurements, especially when detailed analysis of donor fluorescence decay is for any reason difficult.

ACKNOWLEDGMENTS

We thank Arie van Hoek for assistance in the laser experiments and Kees Vos for making available the computer programs for CD and fluorescence decay analysis. We acknowledge Yvonne Soekhram for patiently editing the typescript and Martin Bouwmans for graphical assistance.

Registry No. I, 2535-20-8; II, 17879-89-9; III, 83-88-5; L-Trp, 73-22-3.

REFERENCES

Barkley, M. D., Kowalczyk, A. A., & Brand, L. (1981a) in *Proceedings of the Second SUNYA Conversation in the Discipline Biomolecular Stereodynamics* (Sarma, R. H., Ed.) pp 391–403, Adenine Press, New York.

Barkley, M. D., Kowalczyk, A. A., & Brand, L. (1981b) *J. Chem. Phys. 75*, 3581–3593.

Beechem, J. M., & Brand, L. (1985) *Annu. Rev. Biochem. 54*, 43–71.

Belford, G. G., Belford, R. L., & Weber, G. (1972) *Proc. Natl. Acad. Sci. U.S.A. 69*, 1392–1393.

Birks, J. B. (1979) *Photophysics of Aromatic Molecules*, pp 567–576, Wiley, London.

Cantor, C. R., & Schimmel, P. R. (1980) *Biophysical Chemistry*, Part II, p 426, W. H. Freeman, San Francisco.

Chang, M. C., Petrich, J. E., McDonald, D. B., & Fleming, G. R. (1983) *J. Am. Chem. Soc. 105*, 3819–3824.

Chen, Y.-H., Yang, J. T., & Chau, K. H. (1974) *Biochemistry 13*, 3350–3359.

Chien, Y., & Weber, G. (1973) *Biochem. Biophys. Res. Commun. 50*, 538–543.

Chuang, T. J., & Eisenthal, K. B. (1972) *J. Chem. Phys. 57*, 5094–5097.

Cundall, R. B., & Dale, R. E., Eds. (1983) *Time-Resolved Fluorescence Spectroscopy in Biochemistry and Biology*, Plenum, London.

Dale, R. E., & Eisinger, J. (1974) *Biopolymers 13*, 1573–1605.

Edmondson, D. E., & Tollin, G. (1971) *Biochemistry 10*, 113–124.

Ehrenberg, M., & Rigler, R. (1972) *Chem. Phys. Lett. 14*, 539–544.

Eisinger, J., Feuer, B., & Lamola, A. A. (1969) *Biochemistry 8*, 3908–3915.

Greenfield, N., & Fasman, G. D. (1969) *Biochemistry 8*, 4108–4116.

Gudgin-Templeton, E. F., & Ware, W. R. (1984) *J. Phys. Chem. 88*, 4626–4631.

Haas, E., Katchalski-Katzir, E., & Steinberg, I. Z. (1978) *Biopolymers 17*, 11–31.

Hennessey, J. P., & Johnson, W. C. (1981) *Biochemistry 20*, 1085–1094.

Koenig, S. H. (1975) *Biopolymers 14*, 2421–2423.

Lakowicz, J. R. (1983) *Principles of Fluorescence Spectroscopy*, Plenum, New York.

Lampert, R. A., Chewter, L. A., Phillips, D., O'Connor, D. V., Roberts, A. J., & Meech, S. R. (1983) *Anal. Chem. 55*, 68–73.

Lee, J. (1985) in *Chemi- and Bioluminescence* (Burr, J. G., Ed.) pp 401–437, Marcel Dekker, New York.

Lee, J., O'Kane, D. J., & Visser, A. J. W. G. (1985) *Biochemistry 24*, 1476–1483.

Masotti, L., & Szabo, A. G., Eds. (1987) *Excited State Probes in Biochemistry and Biology*, Plenum, New York (in press).

O'Kane, D. J., & Lee, J. (1985a) *Biochemistry 24*, 1467–1475.

O'Kane, D. J., & Lee, J. (1985b) *Biochemistry 24*, 1484–1488.

O'Kane, D. J., Karle, V. A., & Lee, J. (1985) *Biochemistry 24*, 1461–1467.

Petrich, J. W., Chang, M. C., McDonald, D. B., & Fleming, G. R. (1983) *J. Am. Chem. Soc. 105*, 3824–3832.

Rowan, T., & Wood, H. C. S. (1968) *J. Chem. Soc. C*, 452–458.

Saxena, V. P., & Wetlaufer, D. B. (1971) *Proc. Natl. Acad. Sci. U.S.A. 68*, 969–972.

Small, E. W., & Isenberg, I. (1977) *Biopolymers 16*, 1907–1928.

Steinberg, I. Z. (1971) *Annu. Rev. Biochem. 40*, 83–114.

Szabo, A. G., & Rayner, D. M. (1980) *J. Am. Chem. Soc. 102*, 554–563.

Valeur, B., & Weber, G. (1977) *Photochem. Photobiol. 25*, 441–444.

van Hoek, A., & Visser, A. J. W. G. (1981) *Rev. Sci. Instrum. 52*, 1199–1205.

van Hoek, A., & Visser, A. J. W. G. (1985) *Anal. Instrum. (N.Y.) 14*, 359–378.

van Hoek, A., Vervoort, J., & Visser, A. J. W. G. (1983) *J. Biochem. Biophys. Methods 7*, 243–254.

Visser, A. J. W. G., & Lee, J. (1980) *Biochemistry 19*, 4366–4372.

Visser, A. J. W. G., & Santema, J. S. (1981) *Photobiochem. Photobiophys. 3*, 125–133.
Visser, A. J. W. G., & van Hoek, A. (1981) *Photochem. Photobiol. 33*, 35–40.
Visser, A. J. W. G., & Lee, J. (1987) in *Excited State Probes in Biochemistry and Biology* (Masotti, L., & Szabo, A. G., Eds.) Plenum, New York (in press).
Visser, A. J. W. G., Ykema, T., van Hoek, A., O'Kane, D. J., & Lee, J. (1985) *Biochemistry 24*, 1489–1496.
Wahl, Ph. (1979) *Biophys. Chem. 10*, 91–104.
Weber, G., & Teale, F. W. J. (1957) *Trans. Faraday Soc. 53*, 646–655.
Zuker, M., Szabo, A. G., Bramall, L., Krajcarski, D. T., & Selinger, B. (1985) *Rev. Sci. Instrum. 56*, 14–22.

Nuclear Magnetic Resonance and Molecular Genetic Studies of the Membrane-Bound D-Lactate Dehydrogenase of *Escherichia coli*†

Gordon S. Rule,‡ E. A. Pratt, Virgil Simplaceanu, and Chien Ho*
Department of Biological Sciences, Carnegie-Mellon University, Pittsburgh, Pennsylvania 15213
Received June 17, 1986; Revised Manuscript Received October 2, 1986

ABSTRACT: In this study we demonstrate the potential of combining fluorine-19 nuclear magnetic resonance (NMR) spectroscopy with molecular genetics. We are using the membrane-bound enzyme D-lactate dehydrogenase of *Escherichia coli* as a model system to characterize interactions between proteins and lipids. We have labeled D-lactate dehydrogenase with 4-, 5-, and 6-fluorotryptophans and obtained high-resolution fluorine-19 NMR spectra showing five resonances, in agreement with the five tryptophan residues expected from the DNA sequence. The five ^{19}F resonances in the spectra have been assigned to the specific tryptophan residues in the primary sequence of D-lactate dehydrogenase by site-directed oligonucleotide mutagenesis of the cloned gene. We observe large differences in the relative fluorine-19 chemical shifts of each tryptophan residue when labeled by different isomers of fluorotryptophan. We have determined by NMR methods that two tryptophans are exposed to the solvent and that none of the tryptophan residues are within 10 Å of the lipid phase. On the basis of ^{19}F NMR spectroscopy of the labeled tryptophan residues, the conformation of D-lactate dehydrogenase is similar in aqueous solution and in the presence of a variety of lipids and detergents. This result indicates that the presence of lipids or detergents is not required to maintain the tertiary structure of this membrane-bound enzyme. In contrast, Triton X-100 induces a change to an abnormal conformation of the enzyme as judged from both NMR spectroscopy and the effect of temperature on the maximal velocity of the enzyme in the presence of this detergent.

The biochemical function of a large number of membrane enzymes is well understood. However, the body of information describing structural properties of membrane enzymes is quite sparse. Consequently, it is difficult to describe structure–function relationships for this type of enzyme. To obtain information about biological membranes, our laboratory has been using ^{19}F nuclear magnetic resonance (NMR)[1] techniques to investigate the structure and dynamics of membrane lipids and proteins. For a recent review, see Ho et al. (1985).

As a model system in which to study protein–lipid interactions, we have chosen the membrane-bound enzyme D-lactate dehydrogenase (D-LDH) of *Escherichia coli*. This flavin-containing enzyme has a molecular weight of 65 000 and catalyzes the oxidation of D-lactate in an electron-transfer reaction that is coupled to the active transport of various amino acids and sugars into membrane vesicles (Barnes & Kaback, 1971; Futai, 1973; Kohn & Kaback, 1973). These activities can be reconstituted by the addition of purified enzyme to D-LDH-deficient membrane vesicles (Futai, 1974; Short et al., 1974). The activity of D-LDH is enhanced by a wide variety of lipids and detergents (Fung et al., 1979; Kovatchev et al., 1981). Thus, it is possible to study the properties of D-LDH in the presence of defined, synthetic lipids and detergents.

The gene encoding D-LDH has been cloned (Young et al., 1982), and the nucleotide sequence of the D-LDH gene has also been determined (Campbell et al., 1984; Rule et al., 1985). The availability of the cloned gene has allowed us to combine the techniques of molecular genetics and ^{19}F NMR to investigate protein–lipid interactions in this model system. We have been able to overproduce D-LDH by 300-fold (Rule et al., 1985) and thus obtain sufficient material for the NMR studies described in this paper. In addition, it has also been possible to use site-directed oligonucleotide mutagenesis to assign the ^{19}F resonances. This is accomplished by generating mutant

† This work was supported by a research grant from the National Institutes of Health (GM-26874). G.S.R. was supported by a Predoctoral Training Grant in Cellular and Molecular Biology awarded by the National Institutes of Health (GM-08067). This work was presented in part at the 5th Biophysical Discussion, Nov 10–13, 1985, Airlie House, Airlie, VA, and the Membrane Protein Symposium, Aug 3–6, 1986, San Diego, CA.
* Address correspondence to this author.
‡ Present address: Department of Chemistry, Stanford University, Stanford, CA 94305.

[1] Abbreviations: NMR, nuclear magnetic resonance; D-LDH, D-lactate dehydrogenase; F-Trp, fluorotryptophan; SIIS, solvent isotopic induced shift; $C_{12}E_7$, heptaethylene glycol dodecyl ether (Brij); PMS, phenazine methosulfate; MTT, 3-(4,5-dimethylthiazol-2-yl)-2,5-diphenyltetrazolium bromide; EDTA, ethylenediaminetetraacetic acid; SDS, sodium dodecyl sulfate; DPPG, dipalmitoylphosphatidylglycerol; T_1, spin–lattice relaxation time; NOE, nuclear Overhauser effect; TFA, trifluoroacetic acid; CD, circular dichroism; FAD, flavin adenine dinucleotide.

0006-2960/87/0426-0549$01.50/0